Mapping Weathering and Alteration Minerals in Virginia City, Nevada with AVIRIS and HyperSpecTIR

R. Greg Vaughan[1,2] and Wendy M. Calvin[1]

[1] University of Nevada Reno, Department of Geological Sciences
[2] Present address: Jet Propulsion Laboratory, Pasadena CA (greg.vaughan@jpl.nasa.gov)

1. Introduction

1.1 Virginia City

Situated on the east side of the Virginia Range, Virginia City (Figure 1) is the home of the historic Comstock mining district and was mined as a source of Au and Ag between 1859 and the 1960's, with numerous underground workings and small open pit operations. The Virginia Range consists mostly of Oligocene to Miocene volcanic rocks that overlie Mesozoic metamorphic rocks (Mzvs) and Cretaceous granodiorite (Kgd) (Figure 2). Andesite to dacite flows, breccias and intrusives of the Alta Formation (Ta) (18-15 Ma) (Hudson, 2003) are overlain by intermediate volcanic, volcaniclastic and locally intrusive rocks of the Kate Peak Formation (Tk) (14.7-12 Ma) (Vikre, 1998; Hudson, 2003). Contemporaneous with the Alta Formation was the intrusion of the Davidson diorite (15.2 Ma) (Castor et al., 2002), which forms the bulk of Mt. Davidson just west of the town site. Hydrothermal alteration in the Comstock district is widespread, with several episodes of hydrothermal events and subsequent precious metal mineralization. Alteration mineral assemblages have been distinguished based on their dominant mineral constituents (Hudson, 1987; Hutsinpillar and Taranik, 1988; Vikre et al., 1988; Vikre 1998; Hudson, 2003).

The *alunitic* alteration assemblage consists of alunite + quartz + pyrite; the *alsic* zone consists of pyrophyllite + quartz + diaspore; the *kaolinitic* zone consists of kaolinite + quartz + pyrite; the *illitic* zone consists of illite + montmorillonite (mixed layered) + quartz + pyrite; the *sericitic* zone consists of sericite + quartz + pyrite; and the *propylitic* zone consists of chlorite + albite + epidote + calcite + illite/sericite + quartz + pyrite. Table 1 lists these alteration assemblages with their characteristic mineralogy and also indicates the minerals that display diagnostic spectral features in the VNIR/SWIR wavelength region.

The Alta Formation is generally more altered than the Kate Peak, and the accurate dating of the complex series of magmatic events and pulses of hydrothermal activity and mineralization is the subject of on-going study (S. Castor, pers. comm., 2004). Precious-metal mineralization in the Comstock district is concentrated along major north-northeast trending structures. The Comstock fault, which transects the town site, and the Occidental fault to the east, are two such structures that strike north-northeast, dip steeply to the east, and once provided pathways for mineralizing fluids. Another structural zone to the west of Mt. Davidson, the Jumbo zone (Vikre, 1998), displays acid-sulfate alteration and minor precious metal mineralization in adularia-sericite veins along an east-dipping fault. Recent studies indicate that alteration and mineralization events appear to have shifted from west of Virginia City (Jumbo), to the east (Comstock, then Occidental) with time (Castor et al., 2002; Vikre et al., 2003).

As a historic mining district with over 100 years of activity, much of the surface area in Virginia City (approximately 0.85 km^2) is covered with mine dumps. Mine dumps and tailings piles are composed of minerals like quartz, pyrite, and various clay minerals, and often contain anomalous concentrations of accessory elements such as Hg, As, Cd, Co, Cu, Mo, Ni, Pb, Zn, Se, and Sb. Iron sulfides, most commonly pyrite, exposed at the surface readily oxidize to form secondary Fe-bearing minerals, which are indicative of the chemical conditions under which they form (Swayze et al., 1998; Swayze et al., 2000; Jambor et al., 2000; Bigham and Nordstrom, 2000; Montero et al., 2004). Pyrite oxidation is a complex biogeochemical process involving hydration, oxidation, and microbial catalysis that results in the formation of acidic water (Bigham and Nordstrom, 2000). Acidic surface water, and water that percolates through the porous rock pile, contain dissolved heavy metals and travel away from the acid-generating source. Chemical reactions with other rocks and minerals partially neutralize the pH of the water, which

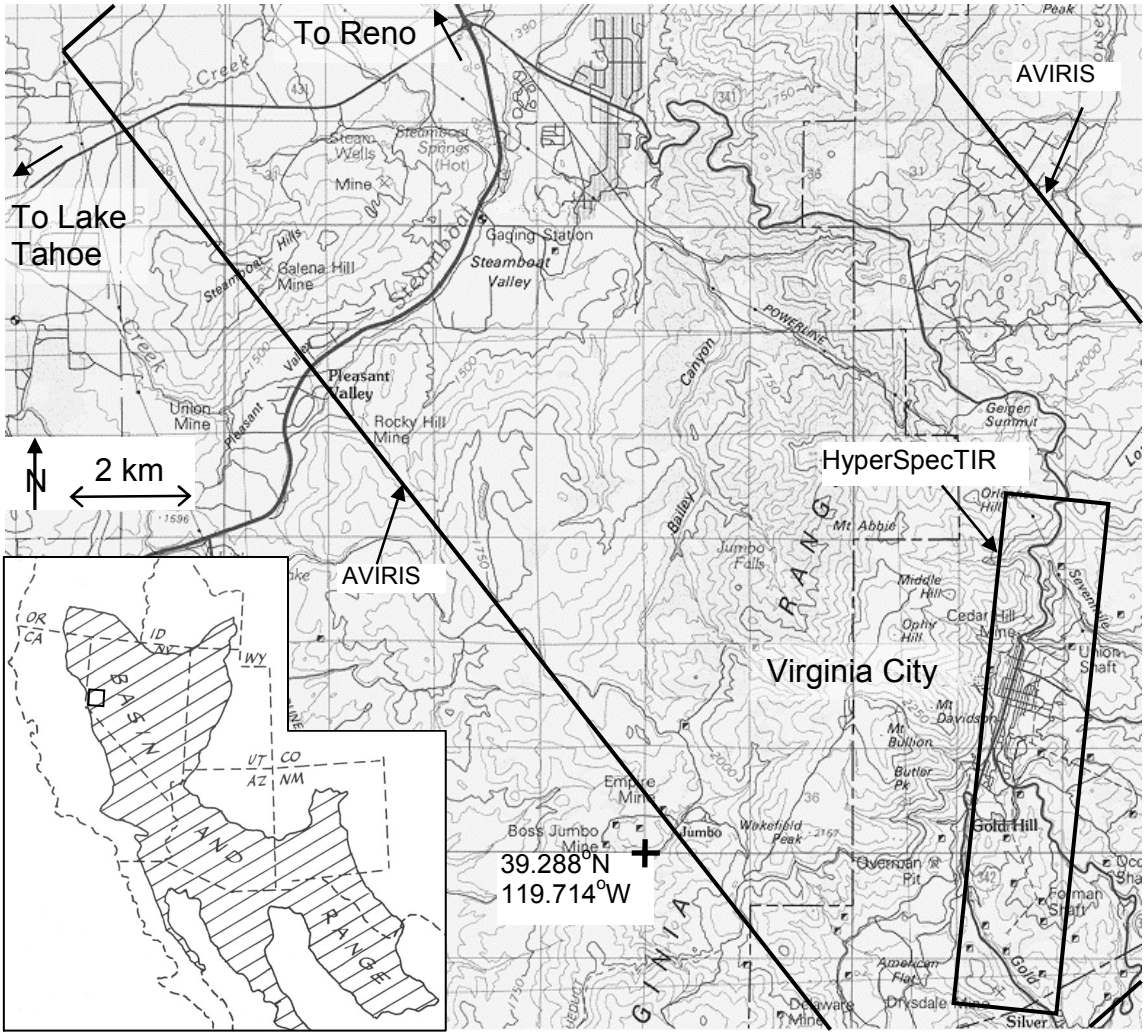

Figure 1. Map showing the location of Virginia City with respect to Nevada and the Basin and Range geologic province. Also shown are the outlines of the AVIRIS and HST data sets acquired. Inset figure from Fiero (1986).

leads to the precipitation of Fe-sulfates (e.g., jarosite, schwertmannite, or copiapite), Fe-oxyhydroxides (e.g., goethite), and Fe-oxides (e.g., hematite) that sometimes forms a spatial pattern around points of actively oxidizing sulfides (Montero et al., 2004). The occurrence of water-soluble sulfates on mine dumps is also indicative of acidic surface conditions. These sulfate salts can contain high concentrations of heavy metals within their crystal structure that can be rapidly released during increased water flow shortly after rainfall events (Jambor et al., 2000; Montero et al., 2004).

1.2. Background and Objectives

With a wide range of exposed weathering and alteration minerals, Virginia City has been the focus of numerous hyperspectral imaging spectroscopy studies (Ashley et al., 1979; Hutsinpillar and Taranik, 1988; Kruse and Huntington 1996; Yang et al., 1999). This study introduces a new hyperspectral imaging spectrometer to the family of sensors that have imaged Virginia City. The SpecTIR Corporation's airborne hyperspectral imager, HyperSpecTIR (HST) has been designed to acquire images with a very high-spatial resolution without significant loss of signal over noise. This

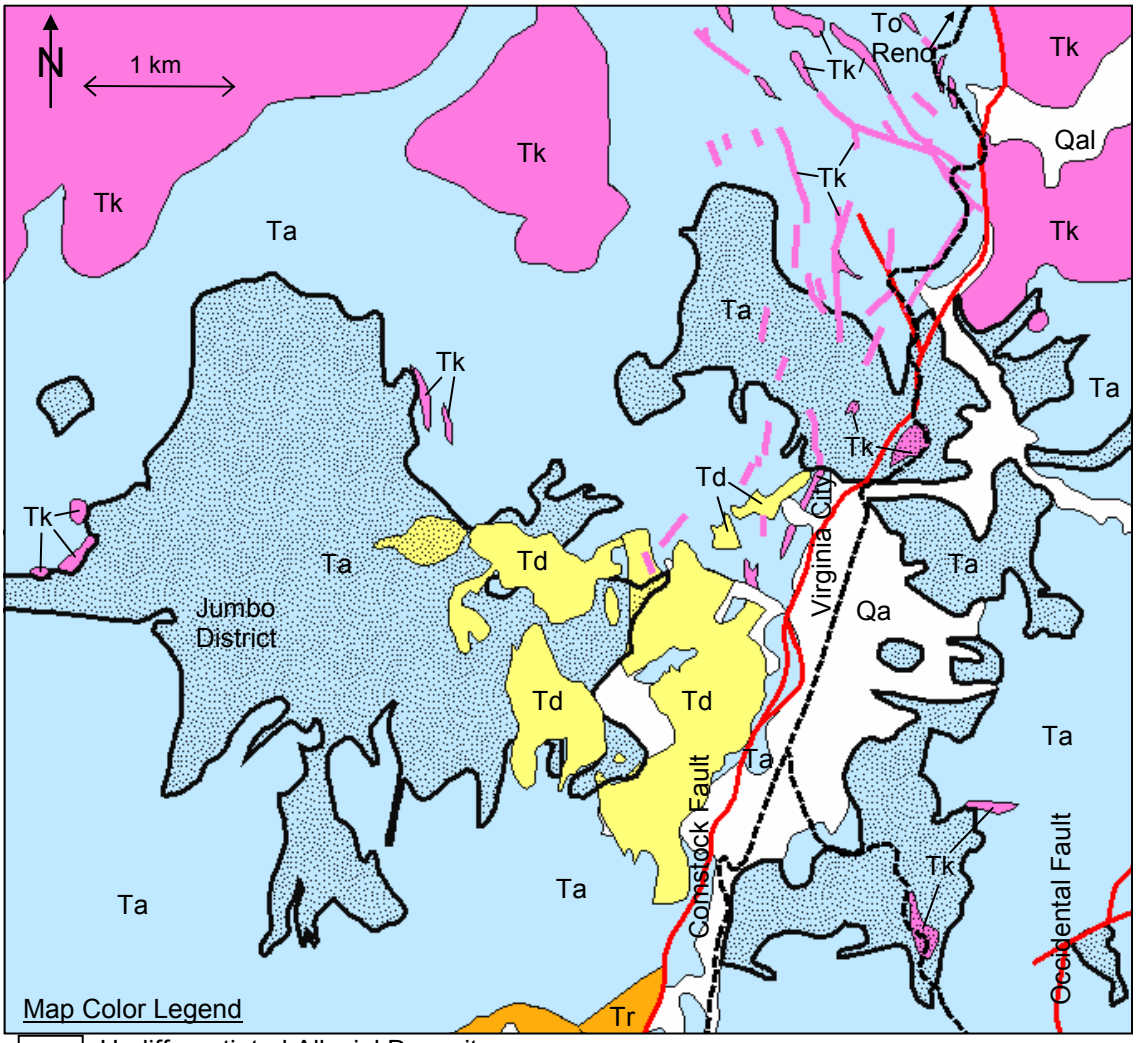

Qal — Undifferentiated Alluvial Deposits

Bleached: Rocks subjected to acid-sulfate type hydrothermal alteration.

Tk — Kate Peak Formation: Lavas, flow breccias, and porphyritic intrusives. Andesite in composition with hornblende, biotite, and pyroxene. 12-15 Ma (Vikre et al., 1988).

Td — Davidson Diorite: Medium-grained intrusive with plagioclase, orthoclase, quartz, and slightly altered ferromagnesian minerals (pyroxene, hornblende, biotite). 15-16 Ma (Vikre et al., 1988)

Ta — Alta Formation: Lavas, pyroclastics, and possibly intrusives. Andesite in composition with hornblende and pyroxene. Hydrothermally altered in many areas. 15-18 Ma (Vikre et al., 1988).

Tr — Hartford Hill Formation: Tuff and tuff breccia with devitrified pumice and glass + quartz, orthoclase, plagioclase and biotite. Rhyolitic in composition.

Roads — Faults — Tk intrusive dikes

Figure 2. Simplified geologic map of the Comstock district and Virginia City (from Thompson and White, 1964; and Hudson, 2003).

study represents the first geological analysis of the new HST data and presents mineral mapping results of one of the highest-spatial resolution hyperspectral data sets acquired over Virginia City.

Table 1. Alteration mineral assemblages in the Geiger Grade and Comstock alteration zones (from Hudson, 1987).

Alteration Type	Mineral Assemblage	Absorption features in the VNIR/SWIR
Alunitic	alunite, quartz, pyrite	alunite
Alsic	pyrophyllite, quartz, diaspore, kaolinite, pyrite	pyrophyllite, diaspore, kaolinite
Kaolinitic	kaolinite, quartz, pyrite	kaolinite
Illitic	illite, quartz, pyrite, montmorillonite	illite, montmorillonite
Sericitic	sericite, quartz, pyrite	sericite
Propylitic	albite, chlorite, epidote, calcite, illite/sercite, quartz, pyrite	chlorite, epidote, calcite, illite/sercite

The purpose of this study was to use both AVIRIS and HST data to map weathering and alteration minerals in the Comstock region and relate the mineral maps to local geology and chemical conditions on the mine dumps. It is instinctive to compare and contrast two data sets with different spatial resolution, but also helpful to use them together to make use of the advantages of each instrument. To what extent do these mineral maps agree with and/or add information to current geologic maps and alteration models of this well-studied region? Is there potential for acid mine drainage from the mine dumps in Virginia City?

2. Data Collection and Atmospheric Correction

AVIRIS data were collected over Virginia City in July 1995 from the high-altitude ER-2 platform and have a swath of ~11 km and a spatial resolution of ~18 m. The signal-to-noise ratio (SNR) of the 1995 AVIRIS data has been reported as >600:1 in the VNIR channels (Swayze et al., 2003), and calculations of SNR from these Virginia City data using the mean/standard deviation method normalized to 50% reflectance yield a SNR of ~500:1 in the VNIR channels.

The HyperSpecTIR (HST) is a hyperspectral imaging spectrometer developed and operated by the Spectral Technology and Innovative Research (SpecTIR) Corporation. It measures solar reflected radiance in 227 continuous spectral channels between 0.45 and 2.45 μm with a spectral band pass that is selectable from 5 to 10 nm. It has an IFOV of 1 mrad and a TFOV that is selectable from 0 to 1 rad (57^o) (Watts et al., 2001). The instrument is mounted on a tilting platform equipped with a "fast optical line-of-sight steering" system that allows for real-time compensation of aircraft motion (roll, pitch and yaw variations) in heavy turbulence (Watts et al., 2001). It also increases the dwell time over the target, thus increasing the amount of incoming signal. The SNR in the VNIR channels calculated using the mean/standard deviation method and normalized to 50% reflectance was ~250:1. Images were acquired in a series of overlapping frames rather than a single, continuous strip. HST data were acquired over Virginia City, Nevada in June 2002 from a Cessna 310 aircraft at an altitude of 2.5 km AGL. The images cover a ground swath of about 1.1 km and have a spatial resolution of ~2.5 m.

For the atmospheric correction of both AVIRIS and HST data a radiative transfer modeling approach was used. For the AVIRIS data, the “fast line-of-sight atmospheric analysis of spectral hypercubes” (FLAASH) method was used (Adler-Golden et al., 1998). The FLAASH method uses the latest version of the “moderate resolution atmospheric radiance and transmission” (MODTRAN) model (Berk et al., 1999) to calculate the atmospheric parameters needed to extract at-surface reflectance. For the MODTRAN calculations the average profile for a typical continental location at mid-latitudes during the summer was assumed. A visibility of 23 km and a typical aerosol profile model for a rural area were also assumed. In addition, a spectral “polishing” routine (using a running average across 9 adjacent channels) was used to eliminate spectral artifacts that remain after atmospheric correction and to account for random channel-to-channel noise (Boardman, 1998; Adler-Golden et al., 1998). For the HST data a similar atmospheric correction method was used that allows MODTRAN to calculate the atmospheric parameters and extract at-surface reflectance. In addition, spectral measurements of natural calibration targets in the field (a recently-paved parking lot, and a large dirt lot) were acquired concurrently with the

HST over flights and compared to image spectra to calculate gain and offset factors for an empirical line correction used to fine-tune SpecTIR's surface reflectance data product.

Retrieved surface reflectance spectra were directly compared to reference spectra for pure minerals that are archived in spectral libraries. Both the USGS and JPL have spectral libraries available via the Internet and contain VNIR/SWIR spectra for over 2000 minerals and rocks combined. The most recent version of the USGS digital spectral library can be found at: http://pubs.usgs.gov/of/2003/ofr-03-395/datatable.html and is described by Clark et al. (2003). The JPL ASTER spectral library is a compilation of spectra of rocks and minerals measured at JPL, JHU, and the USGS, and is described on the Website: http://speclib.jpl.nasa.gov.

Field sites were chosen to aid in the calibration of airborne data sets as well as for the validation of the remotely derived mineral maps. For calibration sites, large (multi-pixel), flat areas that were mineralogically homogeneous and free of vegetation were chosen for field spectrometer measurements. Field sites for validation were also chosen by locating areas in the images that were relatively free of vegetation and thus clearly measured by the remote sensing instrument. An Analytical Spectral Devices (ASD) FieldSpec FR was used in the field for mineral identification and calibration of remote sensing data sets, as well as in the laboratory for high-resolution characterization of field samples (Curtiss and Goetz, 1997). The data were calibrated to reflectance by measuring a dark current to define detector "noise" that contributes to the incoming signal, and by measuring the radiance from a white spectralon® (Labsphere, Inc.) reference panel of known reflectance. X-ray diffraction (XRD) analyses of bulk rock and mineral separate samples were performed at two different laboratories (the Nevada Bureau of Mines and Geology and the University of Georgia) for mineralogical verification.

3. Data Processing and Mineral Mapping

The series of processing steps described by Kruse and Huntington (1996), Kruse et al. (1999), and Kruse et al. (2003) has become standard in hyperspectral data analysis. These methods, shown schematically in Figure 3, yield reproducible results, although there are some subjective decisions required of the user. The purpose of this methodology is to focus only on the information that is relevant to characteristic mineralogic features within the image.

With the AVIRIS data, the MNF transformation was applied to a total of 192 channels of the surface reflectance data that correspond to wavelengths 0.41-1.35, 1.42-1.81, and 1.94-2.48 μm. This

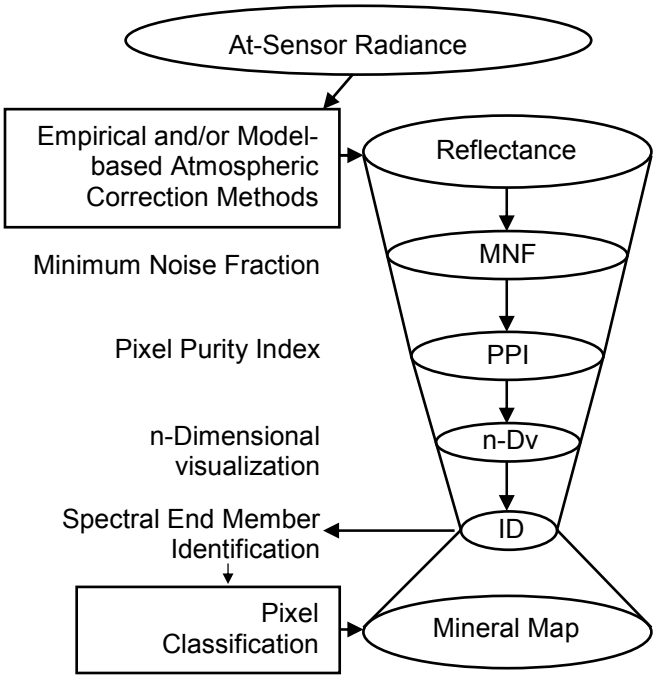

Figure 3. Flow chart illustrating data processing methods. Once the effects of the atmosphere are removed from the at-sensor radiance data, the spectral reflectance information can be extracted. The hyperspectral data processing steps serve to minimize noise and focus on information that is relevant to mineralogic features within the image.

eliminates the strong absorption bands caused by atmospheric H_2O around 1.4 and 1.9 μm. With the HST data, the MNF transformation was applied to a total of 167 channels of the surface reflectance data that correspond to wavelengths 0.49-0.89, 1.16-1.34, 1.43-1.80 and 1.95-2.40 μm. This eliminates the 1.4 and 1.9 μm H_2O bands as well as weak H_2O absorption features around 0.9 and 1.1 μm, which are also present in the HST surface reflectance data.

Reflectance data were used in three ways to find pixels that represent spectral end members. First, Pixel Purity Index (PPI) computation and spectral dimensionality analysis described by Boardman et al. (1995) were used to find spectrally "pure" pixels (target spectra), which represent compositionally distinct areas (Kruse and Huntington, 1996). This significantly reduces the number of pixels that need to be searched for mineralogic spectral information, but it also finds pixels that are not necessarily of geologic interest e.g. urban/ cultural features, and vegetation. The second method is similar, except the pure pixels were chosen by defining regions of interest around obvious geologic targets (e.g., non-vegetated and non-urban areas) and these pixel spectra were viewed as points in n-dimensional space to select the outliers. This helped reduce the number of chosen pixels that were not related to geologic diversity, e.g., vegetation, roads, roofs, and the occasional noisy scan line. Thirdly, spectral end member pixels were chosen based on a priori knowledge and sampling of the field area. In this case, just a few pixels were selected as end member spectra eliminating the need for n-dimensional analysis. Each spectral end member was used as a target spectrum, to "train" the pixel classification method described next.

Pixels were classified using two different supervised classification methods: 1) Spectral Angle Mapper (SAM) (Kruse et al., 1993) and Matched Filtering (MF) (Boardman et al., 1995). SAM classifies pixels together based on their spectral similarity by treating spectra as vectors in n-dimensional space and calculating the angle between them. The threshold angle used was 0.05 radians. MF generates proportional spectral end member abundance maps based on partial unmixing of image target spectra (Boardman et al., 1995). For each end member mapped, a region of interest (ROI) was defined by selecting a threshold range of values from the abundance maps that corresponded to the highest abundance. Each ROI was assigned to a unique color and displayed over a gray-scale image to produce a mineral classification map. The threshold value selection is somewhat subjective and can lead to slight variations in the final mineral map product. Threshold values can be chosen liberally such that many pixels are classified together that are not truly the same, i.e. results in the inclusion of false-positives in the class. Conversely, threshold values can be chosen conservatively, which results in the inclusion of false negatives, i.e. the classification misses some pixels that should be classified. Some background knowledge of the field area and a basic understanding of common geologic models are helpful, but not necessary. In practice, threshold values were chosen more conservatively to reduce the possibility of false-positives and only classify pixels with a high-confidence in the spectral identification. Finally, based on matching the spectra of classified pixels to the spectra of pure minerals from reference libraries, mineralogy was assigned to classified pixel regions to produce mineral maps.

4. Mineral Mapping Results

Around Virginia City, AVIRIS data mapped the hydrothermal alteration minerals alunite, kaolinite, pyrophyllite, montmorillonite/muscovite and chlorite, and also jarosite on some weathered mine dumps (Figure 4, top). In the spectral plots (Figure 4, bottom), four alteration minerals (alunite, pyrophyllite, kaolinite, and chlorite) are identified based on their spectral features between 2.2 and 2.4 μm, and jarosite is identified based on spectral features at 2.26 and μm.

The AVIRIS spectrum from an outcrop on the south side of a hill, in magenta (site 9a - left spectral plot) matches the USGS library reference spectrum for a linear mixture of kaolinite (60%) and hematite (40%). The field spectrum matches the AVIRIS spectrum and XRD data indicate the presence of quartz and kaolinite. The AVIRIS spectrum from an outcrop forming a tall, erosion-resistant knob, in blue (site 9b – left spectral plot) matches the USGS library reference spectrum for a linear mixture of alunite (60%) and cheat grass (40%). The outcrop is relatively small from an aerial perspective and

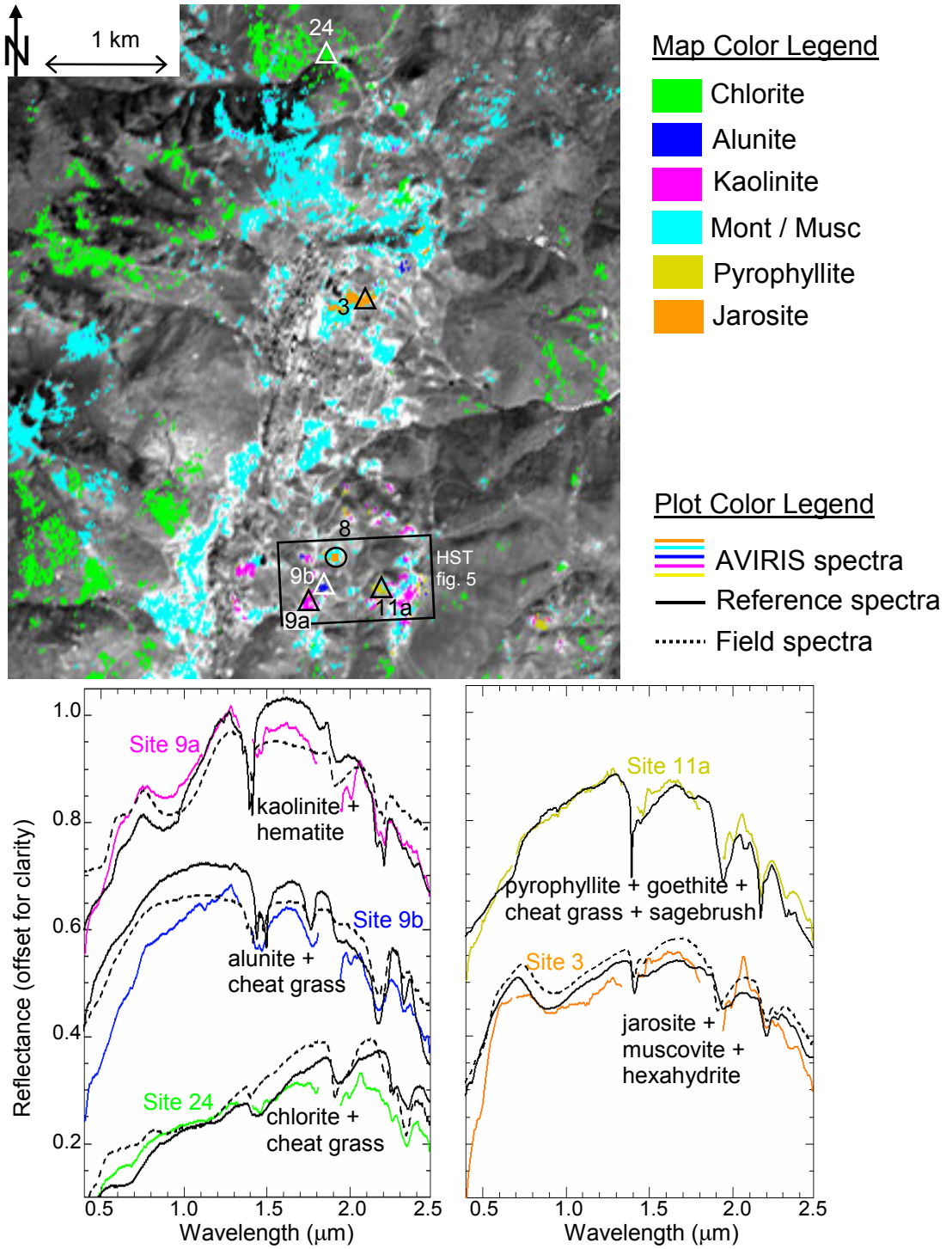

Figure 4. AVIRIS mineral map over Virginia City (top). The five regions mapped are distinguished by their dominant mineralogy and noted in the legend. AVIRIS spectra from representative field sites (3, 9a, 9b, 11, and 24 - marked with triangles on map) are color coordinated to the map legend. The spatial resolution for the AVIRIS image is 18 m.

surrounded by vegetation. The field spectrum matches the AVIRIS spectrum and XRD data from bulk rock samples indicate the presence of quartz, Na-alunite, minamiite, and trace kaolinite. The AVIRIS spectrum from talus material on the side of a hill, on either side of a road cut, in dark yellow (site 11a - right spectral plot) matches the USGS library reference spectrum for a linear mixture of pyrophyllite

(40%), goethite (10%), sage brush (25%) and cheat grass (25%). Based on the narrow feature at 2.17 μm pyrophyllite was identified as the principal clay mineral among an area dominated by vegetation. Bulk rock XRD data from site 11a indicate the presence of quartz, pyrophyllite, and minor kaolinite. The AVIRIS spectrum from a talus slope next to the road, in green (site 24 - left spectral plot) matches the USGS library reference spectrum for a mixture of the chlorite mineral clinochlore (60%) and cheat grass (40%), and corresponds to a zone of propylitic alteration around Virginia City. Clinochlore was identified by the unique spectral feature around 2.34 μm, as well as the very low reflectance below 1.5 μm. The field spectrum matches the AVIRIS spectrum and bulk rock XRD data indicate the presence of quartz, clinochlore, albite, and epidote. Finally, the AVIRIS spectrum from a mine dump, in orange (site 3 - right spectral plot), matches the USGS library reference spectrum for a mixture of jarosite (45%), muscovite (40%) and hexahydrite (15%).

Site 3, as well as other areas mapped in orange (e.g., site 8) are all located on top of mine dumps. Jarosite forms coatings on the rocks around these dumps, and hydrous sulfate salt crusts like hexahydrite and gypsum form in small depressions on top of many weathering mine dumps. The 2.26-μm feature is indicative of jarosite, but this feature is relatively weak as it is mixed with muscovite, which has a stronger feature around 2.20 μm. The presence of jarosite is also implied by the broad 0.9-μm absorption feature and the relatively high reflectance peak around 0.7 μm. However, hematite and goethite also have broad absorption features in the 0.9 μm region, thus the identification of jarosite by AVIRIS with 18-m pixels is somewhat ambiguous. The ASD field spectrum from site 3 matches the AVIRIS spectrum. XRD data from multiple samples of this dump indicate the presence of jarosite, muscovite, quartz, albite, chlorite and white crusts of hydrous Mg-sulfate (hexahydrite), with minor alunogen and gypsum. The dump at site 8 contains dominantly gypsum; the presence of small amounts of gypsum and hexahydrite was identified by field sampling and XRD measurements.

The HST mineral map in Figure 5 (top) is shown to zoom in on a section of Virginia City where there is particularly diverse suite of exposed minerals, including hydrothermal alteration minerals (alunite, kaolinite, montmorillonite/muscovite, and pyrophyllite), as well as a dump containing jarosite and gypsum. In the spectral plot (right), the HST spectrum from the dump, in orange (site 8a) matches the USGS library reference spectrum for a linear mixture of jarosite (40%), muscovite (45%), and gypsum (15%). The ASD field spectrum matches the HST spectrum and XRD data from field samples indicate the presence of quartz, jarosite, and muscovite; and from the sulfate crusts at site 8b, gypsum. The HST spectrum from a resistant outcrop, in blue (site 9b) matches the USGS library reference spectrum for a mixture of alunite (50%), goethite (30%) and cheat grass (20%). XRD data indicate the presence of quartz, Na-alunite, minamiite, and minor kaolinite. The HST spectrum from the talus down hill from a road cut, in dark yellow (site 11a) matches the USGS library reference spectrum for a mixture of pyrophyllite (40%), goethite (40%) and cheat grass (20%). The ASD field spectrum matches the HST spectrum and XRD data indicate the presence of quartz, pyrophyllite, and minor kaolinite. The HST spectrum from an outcrop on a south facing hill, in magenta (site 9a) matches the USGS library reference spectrum for a mixture of kaolinite (55%), hematite (30%) and cheat grass (15%). The ASD field spectrum matches the HST spectrum and XRD data indicate the presence of quartz and kaolinite.

5. Data Interpretation and Discussion

5.1. Hydrothermal Alteration in the Comstock Region

Figure 6 is a mineral map of the Comstock region derived primarily from the AVIRIS data that shows the distribution of large hydrothermal alteration zones. The geologic units from the geology map in Figure 2 are shown in pale, partly transparent colors. The mineral assemblages mapped are shown in solid, opaque colors. Acid-sulfate zones (alunitic, alsic, and kaolinitic assemblages) are shown in magenta, illite/sericite zones in cyan, and propylitic zones in green.

Hydrothermal alteration generally falls within the areas mapped as “bleached” on the original geologic map, and is dominated by widespread propylitic and illitic/sericitic zones, notably on the west

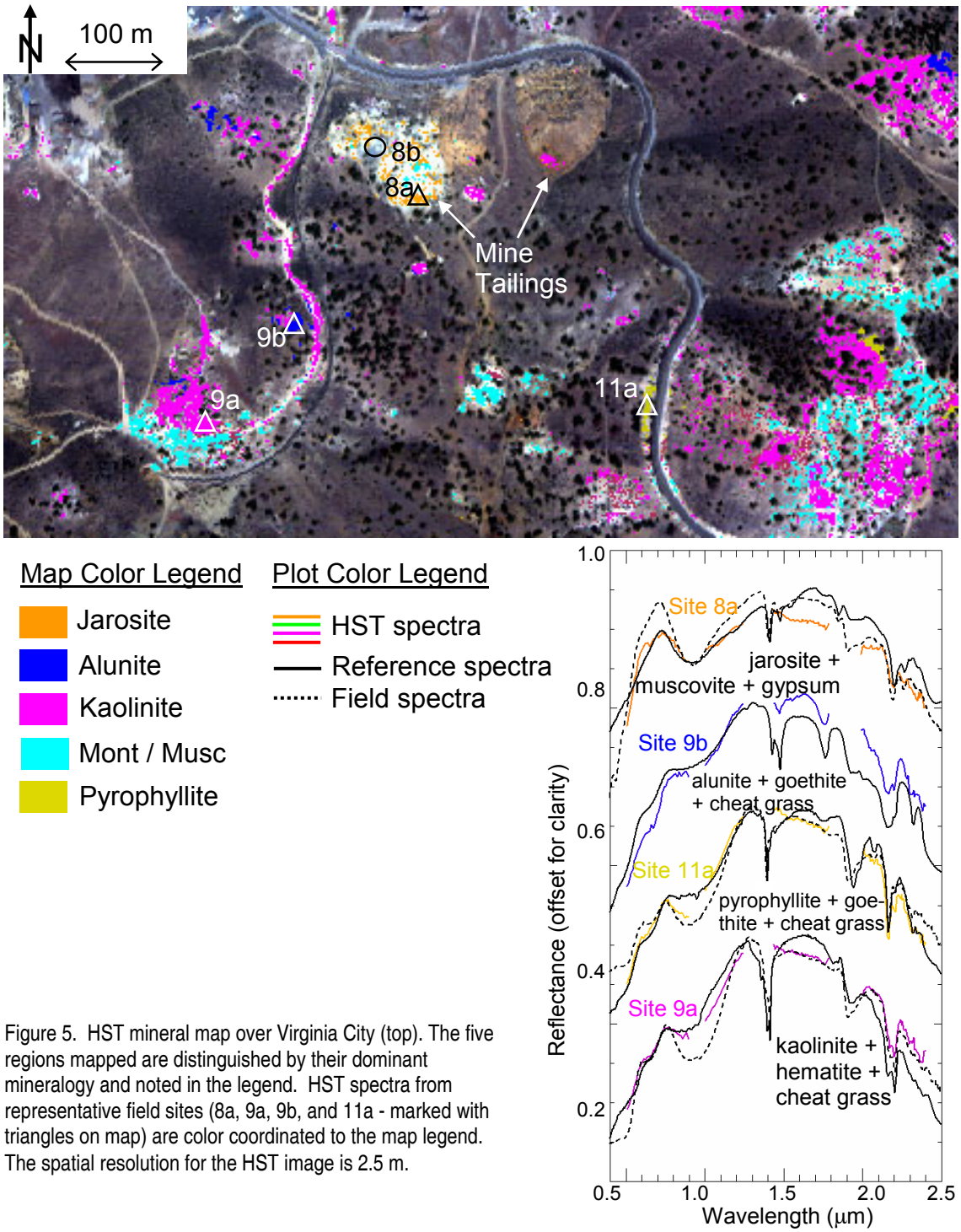

Figure 5. HST mineral map over Virginia City (top). The five regions mapped are distinguished by their dominant mineralogy and noted in the legend. HST spectra from representative field sites (8a, 9a, 9b, and 11a - marked with triangles on map) are color coordinated to the map legend. The spatial resolution for the HST image is 2.5 m.

side (foot wall) of the Comstock fault. Pods of acid-sulfate alteration (alunitic, alsic, and kaolinitic zones) occur on the east side (hanging wall) of the Comstock fault around the Virginia City town site. Also, an acid-sulfate alteration zone (alsic + kaolinitic) is mapped in the hanging wall of the Occidental fault. The areas mapped as "bleached" on the original geologic map generally do not include rocks that are propylitically altered. For example, the Davidson diorite (Td) ranges from relatively unaltered to propylitic and illitic/sericitic alteration in some areas. Other propylitic zones occur along the Comstock and Occidental faults. Hudson (2003) differentiates three different types of propylitic alteration based on

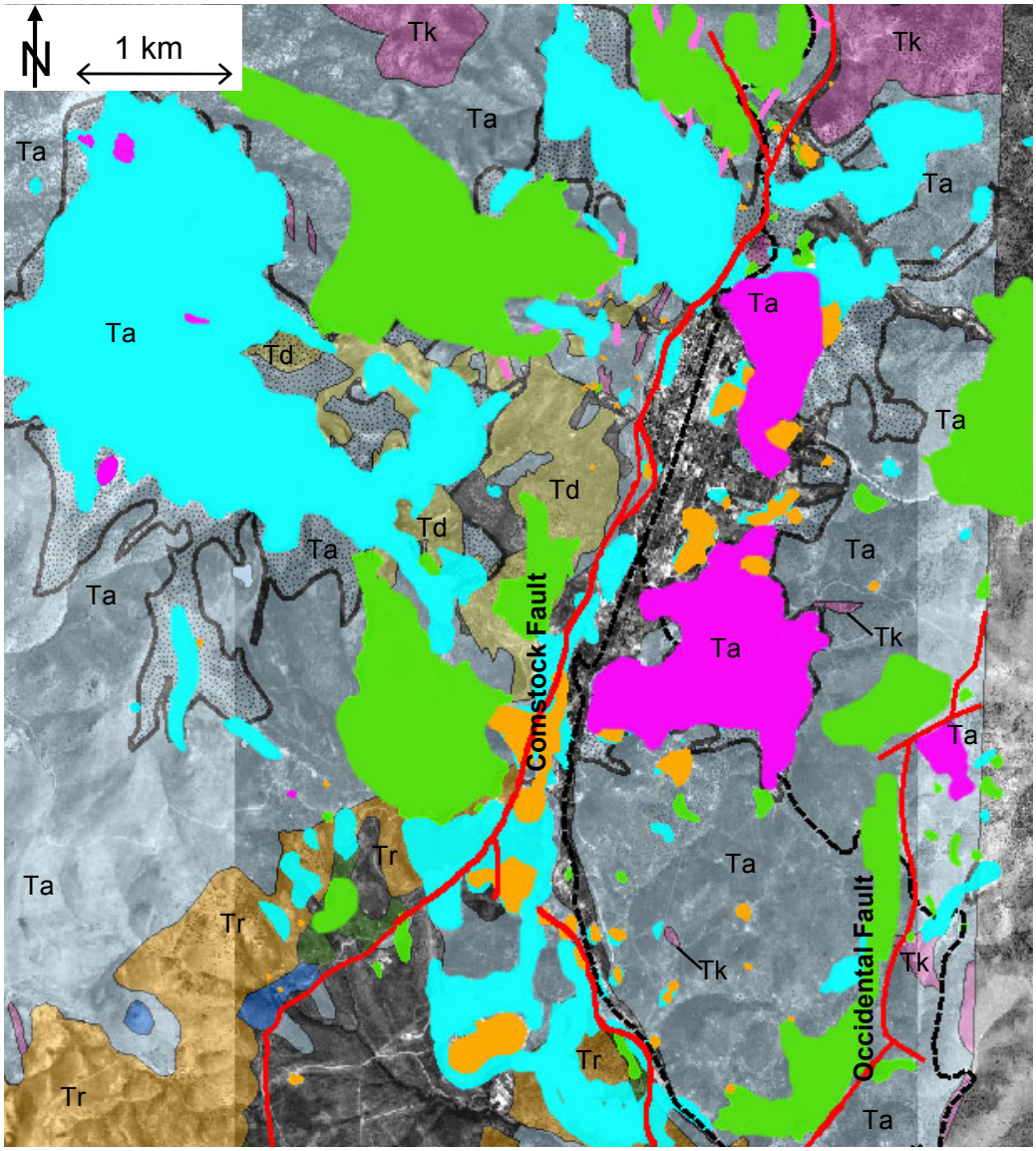

Figure 6. Mineral map of the Comstock district around Virginia City showing the regional-scale distribution of hydrothermal alteration mineral assemblages. The colored lines and polygons are overlain on a gray scale DOQ image.

the relative abundance of epidote, calcite, and albite in the assemblage. Although these minerals were identified by XRD and laboratory spectroscopy, the remote mineral maps classify all propylitic alteration together. The centrality of the Davidson diorite intrusive to intensely altered areas implicates this intrusive body as a heat source (and possibly fluid source) for hydrothermal fluid flow during this time. Geochemical data from these rocks support this assumption, but there may have been other acid-sulfate systems associated with later emplacement of small intrusions and dikes associated with Kate Peak volcanism (Vikre, 1998; Castor et al., 2002; Vikre et al., 2003; Hudson, 2003). In the mineral map it is clear that the widespread propylitic alteration is found in the foot wall blocks of the Comstock and Occidental fault zones, and also proximal to these structures along which mineralized adularia-sericite veins are found. The pervasive acid-sulfate alteration zones, found in the hanging wall blocks, were cut by these younger structures. This is consistent with new radiometric dates from alteration minerals indicate that the acid-sulfate alteration zones pre-date ore-grade mineralization along the Comstock and Occidental faults by ~1-2 million years, and bear only incidental spatial relationship to the ore veins (Vikre et al., 1988; Vikre, 1998; Castor et al., 2002; Hudson, 2003).

Figure 7 is a subset of the Comstock region showing the distribution of alteration mineral zones mapped by HST data on a smaller scale. The rocks here are mostly hydrothermally altered andesite of the Alta Formation (Ta), with one small Kate Peak intrusive plug (Tk) in the southeast part of the image. Several small outcrops of alunitic alteration are mapped (dark blue). These quartz + alunite assemblages are more resistant to erosion and commonly form topographic ridges and small pinnacles (see upper photograph). There are also small resistant pinnacles that are composed of dominantly quartz + kaolinite (see lower photograph) that look very similar. Some of the alunitic zones appear to follow ~northeast-southwest structures, which have not been mapped previously. In agreement with the model of Hudson (1987), the alunitic zones (blue) grade outward into kaolinitic zones (magenta), and then into illitic/sericitic zones (cyan); also, alsic zones rich in pyrophyllite (yellow) grade into kaolinitic and illitic/sericitic zones.

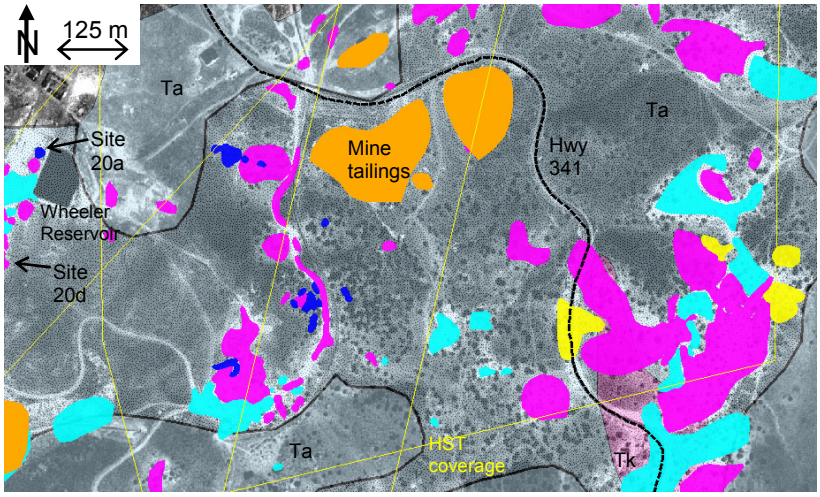

Geologic and Mineral Map Legend

- Tk Kate Peak Andesite
- Ta Alta Andesite
- Bleached Rocks
- Roads
- Faults
- Image Data Coverage
- Illitic/Sericitic Zone
- Kaolinitic Zone
- Alsic Zone
- Alunitic Zone
- Mine Tailings

Site 20a: resistant quartz-alunite outcrop.

Site 20d: resistant quartz-kaolinite outcrop.

Figure 7. Mineral map of an area within Virginia City showing the small-scale distribution of hydrothermal alteration mineral assemblages.

5.2. Secondary Weathering Minerals on Mine Dumps

Figure 8 is a mineral map of the Virginia City area showing the distribution of mine dumps, and some open pit exposures. Jarosite (orange), mapped primarily by the HST data, is indicative of conditions with pH <3 (Montero et al., 2004). Other hydrous sulfate minerals (hexahydrite, alunogen and gypsum) were mapped in the

field and occur as hard, white crusts precipitating in small depressions on top of some of the dumps. The presence of hydrous Ca-Mg-Al sulfate salts on the surface is indicative of pH values between 3 and 5 (C. Alpers pers. comm., 2004). On one dump where both jarosite and hexahydrite had been identified, a pH of 3.5 was measured in a small puddle formed after a recent rain storm. On the edges of the puddle, a white sulfate crust of hexahydrite was beginning to precipitate. This field measurement is in agreement with the range of pH values predicted based on the mapped surface mineralogy.

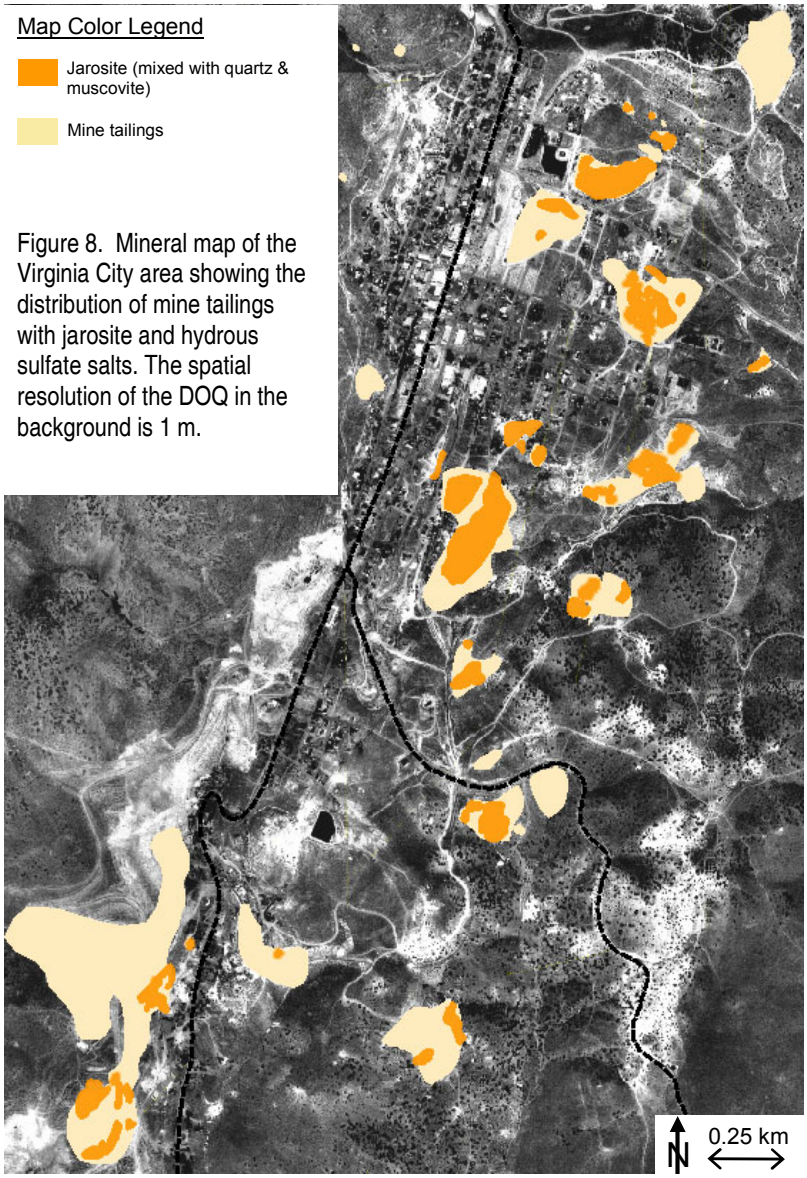

Figure 8. Mineral map of the Virginia City area showing the distribution of mine tailings with jarosite and hydrous sulfate salts. The spatial resolution of the DOQ in the background is 1 m.

Jarosite is considered to be the most important mineral to map to locate potential sources of acid mine drainage. The zoning of goethite and hematite away from oxidizing Fe-sulfide-rich waste rock piles that has been observed by others (Montero et al., 2004; Swayze et al., 2000) is of secondary importance because these minerals can be found in many other environments and are not necessarily indicative of acid drainage potential. For example, the soils and hydrothermally altered volcanic rocks in the surrounding area contain hematite and goethite nearly ubiquitously. The distribution of jarosite on the flanks of the mine dumps and the lack of distal jarosite deposits indicate that acidic waters are confined to the dump environment and not found down stream.

6. Summary and Conclusions

6.1. Weathering and Alteration Mineral Maps

All of the significant base and precious metal deposits in the Virginia Range are located within, or proximal to, acid-sulfate alteration zones in Miocene volcanic rocks (Vikre, 1998). The Comstock region however, appears to be unique. Over a period of ~6 million years multiple episodes of magmatic activity were accompanied by, or followed by, different types of hydrothermal alteration and mineralization. The mineral maps show the distribution of these large alteration zones from which relative timing can be inferred. The maps also show small-scale zoning of alteration minerals. Of particular importance is alunite, which, 1) is an indicator of acid-sulfate systems, 2) tends to delineate structures, and 3) is a hydrous K-bearing sulfate mineral that can be analyzed by a number of geochemical

methods to provide information about the geochemical and temperature environment, and timing of hydrothermal activity.

Of the approximately 0.35 km^2 of tailings piles in Virginia City that were mapped, about 30% of that area contained jarosite mineralization on the surface and an estimated 5% contained water-soluble Mg-, Al- and Ca-sulfate salt deposits. Although no known reports of acid mine drainage problems from the town site have been published, there are clearly acid-generating source materials dispersed around the town site and acidic surface water has been observed after short rainfall events. The acidic source areas identified in this study could serve in future reclamation efforts should acid mine drainage become a serious problem.

6.2. Remote Sensing

The zonation of hydrothermal alteration minerals commonly observed in the field was also evident in the spectral mineral mapping at both large (AVIRIS) and small (HST) scales. The high-altitude AVIRIS data were better for looking at the Comstock alteration zones on a district-wide scale (10x10 km), while the high-spatial resolution HST data mapped some smaller alunite veins in structural orientations not previously recognized, and was more effective than the 18-m AVIRIS data for the detailed mapping of secondary weathering minerals on the mine dumps. It is important to note that the hydrous sulfate salts on the mine dumps were identified in the field and not by remote VNIR/SWIR imaging spectroscopy, and the unique identification of jarosite is sometimes ambiguous due to its mixture with other minerals like muscovite. The fact that HST mapped more jarosite occurrences than AVIRIS is purely a function of the higher spatial resolution. Even though the estimated SNR for the HST data is lower than for AVIRIS, it was still sufficient to uniquely map the important weathering and alteration minerals in this area.

Since HST data were acquired as a series of overlapping frames, one of the challenges to working with the HST data was the lack of geo-coding information and the need to correct and process each HST frame separately to avoid spectral analysis of re-sampled pixels. Mineral map data products were then warped to a 1-m resolution USGS digital orthophoto quad by choosing 30-50 ground control points per frame, and then stitched together. The lack of geo-coding information is unique to this initial 2002 data set, however, and recent improvements to the HST instrument and data products have addressed some these challenges (see http://www.spectir.com). Both high- and low-altitude airborne imaging spectrometer data should continue to occupy distinct and complementary niches for geoscience remote sensing applications.

Acknowledgements

This work was supported by the NASA Graduate Student Researchers Program, the Nevada Space Grant Consortium, and the Arthur Brant Laboratory for Exploration Geophysics. The authors would also like to thank the Spectral Technology and Innovative Research Corporation and the AVIRIS team at the Jet Propulsion Laboratory.

The work described in this paper was performed at the University of Nevada, Reno. Publication support was provided by the Jet Propulsion Laboratory, California Institute of Technology, under a contract with the National Aeronautics and Space Administration.

References

Adler-Golden, S., Berk, A., Bernstein, L.S., Richtsmeier, S.C., Acharya, P.K., and Matthew, M.W. (1998). FLAASH, A MODTRAN 4 Atmospheric Correction Package for Hyperspectral Data Retrievals and Simulation. *Proceedings of the 7th JPL Airborne Earth Science Workshop*, JPL.

Ashley, R.P., Goetz, A.F.H., Rowan, L.C., and Abrams, M.J. (1979). Detection and Mapping of Hydrothermally Altered Rocks in the Vicinity of the Comstock Lode, Virginia City, Nevada, Using Enhanced Landsat Images. *USGS Open File Report*, 79-960, 41 pp.

Berk, A., Anderson, G.P., Bernstein, L.S., Acharya, P.K., Dothe, H., Matthew, M.W., Adler-Golden, S., Chetwynd, J.H. Jr., Richtsmeier, S.C., Pukall, B., Allred, C.L., Jeong, L.S., and Hoke, M.L. (1999). MODTRAN4 Radiative Transfer Modeling for Atmospheric Correction. *Proceedings of the 8th JPL Airborne Earth Science Workshop*, JPL Publication 99-17.

Bigham, J.M. and Nordstrom, D.K. (2000). Iron and Aluminum Hydroxysulfates from Acid Sulfate Waters. Ch 7 in: *Reviews in Mineralogy and Geochemistry*, *v. 40, Sulfate Minerals: Crystallography, Geochemistry, and Environmental Significance*, C.N. Alpers, J.L. Jambor, and D.K. Nordstrom editors, Mineralogical Society of America, Washington, D.C., pp. 351-403.

Boardman, J. W., Kruse, F. A., and Green, R. O. (1995). Mapping Target Signatures Via Partial Unmixing of AVIRIS Data. *Proceedings of the Fifth JPL Airborne Earth Science Workshop*, JPL Publication 95-1 (1), pp. 23-26.

Boardman, J.W. (1998). Post-ATREM Polishing of AVIRIS Apparent Reflectance Data Using EFFORT: A Lesson in Accuracy versus Precision. *Summaries of the 7th JPL Airborne Earth Science Workshop*, JPL Publication 97-21.

Castor, S.B., Garside, L.J., Henry, C.D., Hudson, D.M., McIntosh, W.C., and Vikre, P.G. (2002). Multiple Episodes of Magmatism and Mineralization in the Comstock District, Nevada. *Abstracts with Programs*, Geological Society of America, 34(6), p. 185.

Clark, R.N., Swayze, G.A., Wise, R., Livo, K.E., Hoefen, T.M., Kokaly, R.F., and Sutley S.J. (2003). USGS Digital Spectral Library splib05a. *USGS Open File Report*, 03-395.

Curtiss, B. and Goetz, A.F.H. (1997). Field Spectrometry: Techniques and Instrumentation. *Analytical Spectral Devices FieldSpec^{TM} User's Guide*, Appendix A, pp. 45-62.

Fiero, B. 1986. *Geology of the Great Basin*. University of Nevada Reno Press, Reno, NV.

Hudson, D.M. (1987). Steamboat Springs Geothermal Area, Washoe County, Nevada. In: *Bulk Mineable Precious Metal Deposits of the Western United States*, J.L. Johnson editor, Geological Society of Nevada field trip guidebook, pp. 408-412.

Hudson, D.M. (2003). Epithermal Alteration and Mineralization in the Comstock District, Nevada. *Economic Geology*, 98, pp. 367-385.

Hutsinpiller, A. and Taranik, J.V. (1988). Spectral Signatures of Hydrothermal Alteration at Virginia City, Nevada. In: Bulk Mineable Precious Metal Deposits of the Western United States, Robert W. Schafer editor, Geological Society of Nevada Symposium Proceedings, pp. 505-530.

Jambor, J.L., Nordstrom, D.K., and Alpers, C.N. (2000). Metal-Sulfate Salts from Sulfide Mineral Oxidation. Ch 6 in: *Reviews in Mineralogy and Geochemistry*, *v. 40, Sulfate Minerals: Crystallography, Geochemistry, and Environmental Significance*, C.N. Alpers, J.L. Jambor, and D.K. Nordstrom editors, Mineralogical Society of America, Washington, D.C., pp. 303-350.

Kruse, F.A., Lejkoff, A.B., Boardman, J.W., Heidebrecht, K.B., Shapiro, A.T., Barloon, P.J., and Goetz, A.F.H. (1993). The Spectral Image Processing System (SIPS) - Interactive Visualization and Analysis of Imaging Spectrometer Data. *Remote Sensing of Environment*, 44, pp. 145-163.

Kruse, F.A. and Huntington, J.F. (1996). The 1995 AVIRIS Geology Group Shoot. *Proc. of the Sixth JPL Airborne Earth Science Workshop*, JPL Publication 96-4 (1), Pasadena, CA, pp. 155-164.

Kruse, F.A., Boardman, J.W., and Huntington, J.F. (1999). Fifteen Years of Hyperspectral Data: Northern Grapevine Mountains, Nevada. In: *Proceedings of the 8th JPL Airborne Earth Science Workshop*, JPL publication 99-17, pp. 247-258.

Kruse, F.A., Boardman, J.W. and Huntington, J.F. (2003). Comparison of Airborne Hyperspectral Data and EO-1 Hyperion for Mineral Mapping. In: *Special Issue, IEEE Transactions on Geoscience and Remote Sensing*, 41 (6), pp. 1388-1400.

Montero, I.C., Brimhall, G.H., Alpers, C.N., and Swayze, G.A. (2004). Characterization of Waste Rock Associated with Acid Drainage at the Penn Mine, CA, by Ground-based Visible to Short-wave IR Reflectance Spectroscopy Assisted by Digital Mapping. *Chemical Geology*, in review.

Swayze, G.A., Clark, R.N., Smith, K.S., Hageman, P.L., Sutley, S.J., Pearson, R.M., Rust, R.S., Briggs, P.H., Meier, A.L., Singleton, M.J., and Roth, S. (1998). Using Imaging Spectroscopy to Cost-Effectively Locate Acid-Generating Minerals at Mine Sites: An Example From the California Gulch Superfund Site in Leadville, Colorado. Proceedings of the 7th Airborne Earth Science Workshop, JPL publication 97-21 (1), pp. 385-389.

Swayze, G.A., Smith, K.S., Clark, R.N., Sutley, S.J., Pearson, R.M., Vance, J.S.,. Hugeman, P.L, Briggs, P.H., Meier, A.L., Singleton, M.J., Roth, S. (2000). Using Imaging Spectroscopy to Map Acidic Mine Waste. Environ. Sci. Technol. 34, 47-54.

Swayze, G.A., Clark, R.N., Goetz, A.F.H., Chrien, T.G., and Gorelick, N.S. (2003). Effects of Spectrometer Band Pass, Sampling, and Signal-to-Noise Ratio on Spectral Identification Using the Tetracorder Algorithm. *Journal of Geophysical Research*, 108 (E9), pp. 9-1 - 9-30.

Thompson, G.A. and White, D.E. (1964) Regional Geology of the Steamboat Springs Area, Washoe County, Nevada. *USGS Professional Paper* 458-A, 52 pp.

Vikre, P.G., McKee, E.H., and Silberman, M.L. (1988). Chronology of Miocene Hydrothermal and Igneous Events in the Western Virginia Range, Washoe, Storey, and Lyon Counties, Nevada. *Economic Geology*, 83, pp. 864-874.

Vikre, P.G. (1998). Quartz-Alunite Alteration in the Western Part of the Virginia Range, Washoe and Storey Counties, Nevada. *Economic Geology*, 93, pp. 338-346.

Vikre, P.G., Garside, L.J., Castor, S.B., Henry, C.D., Hudson, D.M., and McIntosh, W.C. (2003). Multiple Episodes of Magmatism, Quartz-Alunite Alteration, and Adularia-Sericite Precious Metal Mineralization, Western Virginia Range, Nevada. *Abstracts with Programs*, Geological Society of America, 35 (6), p. 401.

Watts, L.A., Davis, R.O., Granneman, R.D., LaVeigne, J.D., Chandos, R.A., Russell, E.E., and Cairns, B. (2001). Unique VISNIR-SWIR Hyperspectral and Polarimeter Measurements. In: *Proceedings of the 5th Airborne Remote Sensing Conference*, San Francisco, CA.

Yang, K., Huntington, J.F., Boardman, J.W., and Mason, P. (1999). Mapping Hydrothermal Alteration in the Comstock Mining District, Nevada, Using Airborne Hyperspectral Data. *Australian Journal of Earth Sciences*, 46, pp. 915-922.